Data Related to Late Quaternary Surface Faulting on the Eastgate Fault, Churchill County, Nevada

By Anthony J. Crone,[1] Jai-Bok Kyung,[2] Michael N. Machette,[1] David J. Lidke,[1]
Koji Okumura,[3] and Shannon A. Mahan[1]

Pamphlet to accompany Scientific Investigations Map 2893

[1]U.S. Geological Survey, Denver, CO 80225
[2]Korea National University of Education, Chungbuk, South Korea
[3]Hiroshima University, Hiroshima, Japan

U.S. Department of the Interior
U.S. Geological Survey

Contents

Figures

Tables

Data Related to Late Quaternary Surface Faulting on the Eastgate Fault, Churchill County, Nevada

By Anthony J. Crone,[1] Jai-Bok Kyung,[2] Michael N. Machette,[1] David J. Lidke,[1] Koji Okumura,[3] and Shannon A. Mahan[1]

Introduction

In the past 130 years, 11 large (M>6.5) historical earthquakes in the Basin and Range province of the Intermountain West have produced documented surface ruptures (dePolo and others, 1991), the majority of which have occurred in the north-south-trending Central Nevada seismic belt (CNSB; Wallace, 1984a). Slip rates on individual normal-slip faults in the province are low compared to the rates on faults associated with plate boundaries, such as those in California. Nevertheless, these low-slip, normal faults can pose a significant seismic hazard, especially in urbanized areas such as the Wasatch Front in Utah, and the eastern side of the Sierra Nevada Mountains in western Nevada and eastern California.

For the entire Basin and Range province, the concentration of historical surface-faulting earthquakes in the CNSB is anomalous (Wallace, 1984a) and raises many questions about the mechanics, the distribution, and the release of extensional strain in the crust, as well as the temporal and spatial patterns of past earthquakes throughout the province, and locally in the CNSB. As part of regional studies of paleoseismology in the northern Great Basin, we are studying selected major extensional Quaternary faults in a representative transect across the province between Reno, Nev., and Salt Lake City, Utah, at latitudes 39°–41° N. to develop a more comprehensive geologic perspective of strain release from surface-rupturing earthquakes. Recent geodetic studies in this same region indicate that about 11±2 mm of north-northwest-directed extension is occurring in the transect (Bennett and others, 1998; Thatcher and others, 1999), yet there is little quantitative data to indicate just how this strain is being partitioned and has been released in the recent geologic past.

Numerous published reports document the paleoseismic history of faults that have had historical surface rupture in the CNSB (that is, Bell and Katzer, 1990; Wallace, 1984a, b; Caskey and others, 1996; Bell and others, 1999), but little is known about the number and age of prehistoric surface-rupturing earthquakes on the hundreds of Quaternary faults adjacent to the CNSB (fig. 1). We studied the Eastgate fault in west-central Nevada (fig. 2) to help fill this information gap; our study is one of several companion studies of Quaternary faults in nearby parts of the province (Personius and others, 2004; Machette and others, 2005).

The purpose of this map and report is to provide a basic description of the Eastgate fault study and to release the field data that were collected during our study. Much of this detailed information is inappropriate for publication in professional journals, so we use this large-format map and report as a means to release these details to the scientific community. By design, this report contains minimal interpretation of the fault's late Quaternary movement history; this history will be the subject of a future report in a scientific journal.

Regional and Local Setting

The Eastgate fault is located in the high desert of the Basin and Range province of west-central Nevada. The area's arid to semi-arid climate is suitable primarily for grazing cattle, although locally irrigated tracts of land are used to raise hay and feed for the cattle. The terrain consists of generally elongate, rugged mountain blocks separated by broad, low-relief, alluvial basins (fig. 3). In the vicinity of the Eastgate fault, the mountain blocks expose mainly Tertiary volcanic and sedimentary rocks and small areas of Paleozoic sedimentary rocks (fig. 4). Most of the Tertiary volcanic rocks are upper Oligocene to lower Miocene ash-flow tuffs, welded tuffs, and volcanic breccias that erupted from multiple calderas in the region (McKee and Stewart, 1971). These volcanic rocks are overlain by middle to upper Miocene sedimentary rocks that contain tephra layers (Stewart and others, 1999). Broad alluvial piedmonts, presumably of various Quaternary ages, extend basinward from the flanks of the ranges. Modern ephemeral drainages are incised into these piedmont deposits and carry runoff into playas and former pluvial lakes that are located in the center of many valleys. Deflation of the playas and lake deposits has added significant amounts of eolian silt

[1]U.S. Geological Survey, Denver, CO 80225
[2]Korea National University of Education, Chungbuk, South Korea
[3]Hiroshima University, Hiroshima, Japan

to the Holocene and upper Pleistocene alluvial deposits in the surrounding region.

Late Quaternary movement on the Eastgate fault has formed a west-facing scarp, which is prominent near the settlement of Eastgate (figs. 2, 3, and 4). U.S. Highway 50 crosses the scarp about 95 km east of Fallon, Nev., and about 4.5 km south-southwest of Cold Springs Station, Nev. (figs. 1 and 3). The fault bounds the southern and western sides of a series of low hills and cuts a broad alluvial piedmont directly south of the Clan Alpine Mountains and west of the Desatoya Mountains (fig. 4). The fault is about 25–30 km east of the Dixie Valley and Fairview Peak areas, where two major earthquakes produced large surface ruptures on December 16, 1954 (Caskey and others, 1996). The Eastgate is one of many faults in the region that show evidence of late Pleistocene (130–10 ka) or Holocene (<10 ka) faulting (Dohrenwend and others, 1992).

The Eastgate fault is about 12 km long (fig. 3) and forms scarps of differing heights on Quaternary deposits of differing ages, indicating recurrent Quaternary movement. In the vicinity of Eastgate (fig. 4), Quaternary alluvium on the downthrown, west side of the fault is juxtaposed against Tertiary volcanic rocks on the upthrown, east side. Elsewhere along the fault, a prominent scarp is present on Quaternary deposits. On Holocene deposits, the scarp is typically 1–2 m high (fig. 5; table 1, profiles 2 and 6), whereas on older (middle Pleistocene?) deposits, 8-m-high scarps are common (fig. 5; table 1, profiles 5A–C and 7).

The only reported late Quaternary slip rate on the Eastgate fault is given by dePolo (1998), who offers an estimated slip rate on the order of 0.2 mm/yr. (In dePolo's compilation, the Eastgate fault is listed as the "Eastern Edwards Creek Valley fault–MI4C)". His slip-rate estimate is based on a methodology that evaluates the height of faceted spurs in the footwall of the fault, which could reflect a slip rate that spans Neogene time or longer. This slip rate is not based on detailed field studies of Quaternary fault scarps and thus may not represent the late Quaternary rate. A key objective of our work was to characterize the fault's late Quaternary behavior and determine a field-based estimate of the late Quaternary slip rate.

Methods of Study

In 1996, T.P. Barnhard (then with the U.S. Geological Survey) and P.M. DeMartini (Istituto Nazionale di Geofisica e Vulcanologia, Rome, Italy) conducted a reconnaissance of the Eastgate fault and measured seven profiles of the scarp (table 1). Their reconnaissance work showed that large scarps are present on old alluvium, and small scarps are present on young alluvium, which is probably Holocene in age. These relations demonstrate that multiple Quaternary surface-rupturing events have occurred on the fault, and based on this information, we identified the fault as a potential target for detailed studies. A

Table 1. Summary of scarp-profile data for the Eastgate fault, Nevada.

[SH, scarp height; SO, surface offset; θ_m, maximum slope angle. Scarp height and surface offset are measured following the definitions of Bucknam and Anderson (1979). The data for profiles 2C, 3, 4, and 6–9 were collected during reconnaissance studies by T.P. Barnhard and P.M. DeMartini in 1996, using a stadia rod and Abney level. Data for all other profiles were collected by the authors in 2002, using an electronic distance measuring (EDM) instrument. Profiles 1A–1C were measured in the vicinity of the northern trench; this area is labeled as P-1 on figures 2 and 3. Profiles 2A–2C were measured in the vicinity of a small graben (P-2 on figures 2 and 3). Profiles 5A–5C were measured in the vicinity of the central trench (P-5 on figures 2 and 3)]

Profile number	SH (m)	SO (m)	θ_m, degrees	Comments
1A	5.9	5.3	15.6	At northern trench site NEG
1B	6.1	5.4	15.5	About 10 m northwest of NEG; not shown in fig. 5
1C	2.7	2.5	12.2	About 30 m southeast of NEG; not shown in fig. 5
2A	1.6	1.3	10.3	West profile across graben about 250 m southeast of NEG
2B	1.2	1.0	9.1	East profile across graben about 350 m southeast of NEG; not shown in fig. 5
2C	1.0	0.6	7.3	Unpublished data of Barnhard and DeMartini (1996); not shown in fig. 5
3	3.5	1.7	13.0	Unpublished data of Barnhard and DeMartini (1996); unusual morphology
4	2.3	1.7	10.9	Unpublished data of Barnhard and DeMartini (1996)
5A	6.6	6.1	17.8	At central trench site CEG
5B	6.9	5.9	16.6	About 50 m north of CEG; not shown in fig. 5
5C	5.3	4.8	23.8	About 30 m south of CEG; not shown in fig. 5
6	1.5	1.2	14.6	Unpublished data, Barnhard and DeMartini (1996)
7	8.6	7.3	20.6	Unpublished data, Barnhard and DeMartini (1996)
8	2.1	1.7	12.7	Unpublished data, Barnhard and DeMartini (1996)
9	1.4	1.1	14.0	Unpublished data, Barnhard and DeMartini (1996)

more complete history of Quaternary movement on the Eastgate fault would provide a valuable perspective on tectonics in the CNSB, particularly because of the fault's close proximity to the nearby 1954 ruptures in Dixie Valley, at Fairview Peak, and at Rainbow Mountain.

We performed additional reconnaissance work in 2001, and identified several sites where we felt that exploratory trenching could help define the fault's history of late Quaternary movement. Because some of the fault lies within the Bureau of Land Management's (BLM) Wilderness Study Areas (WSA), all potential trenching sites had to be outside of the WSA, as well as in close proximity to existing roads on BLM property. We eventually selected one site near the northern end of the fault (fig. 2; north trench site, NEG), where the scarp is 5.9 m high (table 1; fig. 5*A*, profile P-1A), and a second site near the central part of the fault (fig. 2; central trench site, CEG), where the scarp is 6.6 m high (table 1; fig. 5*A*, profile P-5A). At both sites, the scarps appeared to be little modified by human activity or by recent erosion or deposition. We did not consider sites along the southern part of the fault in the vicinity of Eastgate because, in this area, the faulting juxtaposes Oligocene and Miocene volcanic rocks against Quaternary deposits. This type of setting eliminates the opportunity to correlate deposits across the fault zone, which significantly reduces one's ability to resolve details of the fault's rupture history.

On the basis of our reconnaissance of the two trench sites, we expected to expose stratigraphy that would document the fault's recent movement history. For studies of Quaternary faulting, it is best to excavate sites where fault-scarp colluvium is juxtaposed against Quaternary deposits and where there is hope of correlating deposits across the fault, thus permitting measurement of the total stratigraphic throw, as well as the throw associated with individual earthquakes.

The morphology of single-event fault scarps formed on alluvium can provide a first-order estimate of the scarp's age (Wallace, 1977; Bucknam and Anderson, 1979; Mayer, 1984), although many variables affect the resolution of the resulting age estimates (Pierce and Colman, 1986; Machette, 1989). In general, for scarps of similar height, younger scarps have steeper maximum slope angles; fault scarps degrade as they age, thus reducing their maximum slope angle. The morphology of scarps of known age can be compared to that of undated fault scarps to estimate their age. This comparison is made by plotting a scarp's height against its maximum slope angle, as shown in figure 5*B*.

The scarp-profile data that we have for the Eastgate fault include the data of Barnhard and DeMartini and profiles that we measured using a Sokkia total station (laser distance-measuring theodolite, that is, EDM) in the vicinity of the trench sites. Near the trench sites, we measured one profile along or adjacent to each trench and companion profiles a few tens of meters on either side of the trenches (table 1). Comparing the Eastgate scarp-profile data with linear regressions of scarp-profile data from the Lake Bonneville high-stand shoreline and selected fault scarps in Utah provides useful calibration lines for estimating the morphological age of the Eastgate scarps (fig. 5*B*). The Fish Springs scarps are thought to have an age of about 2 ka, the Drum Mountains scarps about 7–10 ka, the Lake Bonneville shoreline about 14.5 ka, and the Panguitch scarps on the order of 100 ka (Bucknam and Anderson, 1979; Machette, 1989). The Eastgate fault scarp-profile data have considerable scatter but are concentrated between the regression lines for the Drum Mountains and Panguitch scarps, which implies that, based on their morphology, they are older than 7–10 ka. However, there are numerous limitations to assigning ages to fault scarps based solely on their morphology (Machette, 1989), so these estimates should be considered cautiously.

Following archaeological and biological evaluations of the sites, we received BLM approval to trench the scarps at the two sites. The trenches were excavated with a large track-mounted excavator in early September 2002. The trench at the northern (NEG) site was about 22 m long and a maximum of 3.7 m deep (fig. 6). At this site, we also excavated a second smaller, shallower trench, but our brief study of this trench indicated that it would not provide additional information that could not be obtained from the longer, deeper trench. Therefore, we focused our efforts on the larger trench at this site. The trench at the central (CEG) site was more than 26 m long and also had a maximum depth of about 3.7 m (fig. 7). In both trenches, we excavated benches on one side for safety and for improved visibility, and mapped the opposite wall, which remained near vertical. At both sites, we also excavated 2-m-deep pits, 10–15 m upslope from the upper ends of the trenches on the unmodified or eroded upthrown surfaces of the scarps to expose the soils that have formed in the faulted alluvium (table 2). Soil properties provide a general gauge of the alluvium's age by comparing the characteristics of the soils exposed in the pits with similarly developed soils whose age is known (Birkeland, 1999).

To map the trenches, we first removed loose debris and sediment that had been smeared on the wall during excavation. Next, we established horizontal and vertical datums using the EDM and installed string lines attached to spikes to mark the datums. The precision of the EDM permitted us to survey these datums to an accuracy of a few millimeters. We then marked significant stratigraphic contacts, faults, and fractures using small pieces of colored surveyor's flagging attached to pins (small nails). Different colors of flagging corresponded to specific stratigraphic contacts or notable structural features, such as faults and fissures. We mapped the north- or northwest-facing walls because they remained out of direct sunlight for most or all of the day; full or partial sunlight on the walls makes it difficult to see subtle details that commonly provide vital information. To create the trench map, we used the EDM to measure the vertical and horizontal coordinates of each pin and plotted those coordinates onto metric-gridded paper at a scale of 1:25. The pin locations provided precise, closely spaced control points on the trench map and allowed accurate sketching of all stratigraphic and structural features in the trench. From such precisely controlled maps, we can

Table 2. Field properties of relict soils formed in alluvium on stable surface in footwall block at trench sites on the Eastgate fault, Nevada.

[Soil colors are from the Munsell soil color charts (Kollmorgen Instrument Corp., 1994). For details of typical soil properties and terminology, see Birkeland (1999). Soil structure abbreviations are: P, platy; SBK, sub-angular; B, blocky; SG, single grain; M, massive. LB, lower boundary of soil horizon]

Northern (NEG) site

Soil horizon	Depth below surface (cm)	Color (<2 mm fraction) (d, dry; m, moist)	Texture; consistence	Estimated percent gravel; avg. diameter (cm)	Structure	Soil carbonate stage	Comments
Av	0–8	10 YR 7.5/3 (d) 10 YR 5/3 (m)	Silt loam; slightly hard	2–3%; 0.5	P	None	LB–abrupt, smooth; abundant 1–3 mm vesicles.
Bt	8–18	10 YR 5.5/4 (d) 10 YR 5/6 (m)	Gravelly loam; loose	35%; 0.5–2	SBK-B	I	LB–clear, smooth; thin clay films on grains, discontinuous films in pores.
2Btk	18–37	10 YR 7/5 (d) 10 YR 6/4.5 (m)	Very gravelly sandy loam; loose	75%; 3–5	SBK-B	I+	LB–clear to gradual, wavy; carbonate coats on base of all clasts, some clasts completely coated.
2Bk	37–75	10 YR 7/3 (d) 10 YR 5/3 (m)	Very gravelly loamy sand/ sandy loam; loose	85%; 3–10	SG	I+ to II-	LB–gradual, wavy; many clasts completely coated with carbonate, locally matrix is white from carbonate.
2Cn	75–94	10 YR 7/25 (d) 10 YR 4/3 (m)	Gravelly loamy sand; loose	60–80%; 3–10	SG	I-	LB–gradual; minor carbonate on bottom of clasts could be pedogenic or deposited by groundwater.
2Ck[1]	94–170+		Gravelly loamy sand; loose	60–80% 3–10	SG	II+ to III	Contains pervasive carbonate that could be deposited by groundwater.

Central (CEG) site

Soil horizon	Depth below surface (cm)	Color (<2 mm fraction) (d, dry; m, moist)	Texture; consistence	Estimated percent gravel; avg. diameter (cm)	Structure	Soil carbonate stage	Comments
Av	0–15	10 YR 6.5/3 (d)	Loam	>10%; 0.5	P	None	LB–sharp, smooth; abundant 0.5 mm vesicles.
Bt	15–36	10 YR 5/4 (d) 10 YR 4/4 (m)	Sandy clay loam; loose	5–10%; 1–2	SBK-B	None	LB–clear, wavy; weak clay films on grains and pores.
Btk	36–47	10 YR 6/6 (d)	Sandy loam to loam	10–15%; 1–3	SBK-B	I	LB–irregular because of change in parent material.
2Bk	47–105	10 YR 8/1.5 (d) 7.5 YR 5/6 (m)	Sandy loam to sand; firm	30–40%; 2–3	P	II+ to III	LB–sharp, smooth; about one-third of volume is $CaCO_3$.
3Bk	105–160	10 YR 8/3 (d) 10 YR 4/4 (m)	Loamy sand; loose to firm	50%; 5–10	SG to M	II	LB–sharp, wavy; debris flow, contains loose sandy layers and firm silty layers.
4Cn	160+		Gravelly sand; loose	75% 3–10	SG	None	No carbonate visible

[1] The carbonate in this horizon was probably deposited by groundwater and is not pedogenic in origin. Therefore, the “k” subhorizon designation for this part of the profile is not formally appropriate, but is used here to signify that an abundant amount of post-depositional carbonate is present in this deposit.

confidently measure the thickness of stratigraphic units and the vertical offset across faults, both of which are important in developing an interpretation of the faulting history.

In both trenches, we collected a limited number of samples for luminescence dating to help establish age constraints on the times of faulting events. Once we identified suitable sampling points, we augered ≈13-cm-diameter horizontal holes into the wall to a depth of about 50–60 cm. In the auger hole, we measured the *in situ* radiation (that is, dose rate) using a field scintillometer for a duration of 999 seconds (maximum allowed by this particular instrument). We made triplicate measurements in each hole and averaged the counts to determine the final *in situ* dose rate for each sample. We then collected the actual luminescence sample by hammering an approximately 10-cm-diameter cylindrical tube at least 10–15 cm deep into the back of the augered hole. We extracted the sample from the hole while under a light-proof, black curtain, immediately wrapped it in several layers of black plastic, and sealed it tightly. We collected three samples for luminescence dating from the northern trench and six samples from the central trench (figs. 6 and 7). Age estimates for the samples were determined using three different luminescence techniques: thermoluminescence (TL), infra-red luminescence (IRSL), and blue-light optically stimulated luminescence (OSL), and each sample was analyzed multiple times. Table 3 summarizes the age estimates of individual analyses for each sample using the various techniques. Some samples yielded consistent results for the differing techniques, whereas the results for other samples were quite variable. Table 4 lists our preferred ages for the samples, which are shown in figures 6 and 7. The precise moisture history for each sample is difficult to estimate; we used an average saturation value of 15 percent for the sample's history.

Next, we systematically photographed the trench walls and, lastly, backfilled the trenches to restore the ground surface to its original morphology.

Description of the Trenches

Northern Trench (NEG)

The NEG trench was excavated across a 5.9-m-high scarp (fig. 8; fig. 5*A*, profile P-1A) that is located at the southwest base of a series of low hills comprised of Oligocene and Miocene silicic ash-flow tuffs and rhyolitic flows (Stewart and Carlson, 1976; Stewart and others, 1999). The trench was located at lat 39°22.825′ N., long 117°52.302′ W. (UTM 11S. 0424923 m E., 4359355 m N.). Most of the throw in the trench was confined to a single, down-to-the-west, normal-slip fault zone (between 9 and 11 m on horizontal scale trench map, fig. 6) (fig. 9), although a small amount of down-to-the-west, normal slip occurred on a secondary fault strand (near 7 m horizontal). The hanging wall of the fault contained numerous anastomosing fractures that had little or no detectable vertical displacement.

Deposits on the upthrown side of the fault consist from bottom to top of a moderately consolidated, well-stratified sequence of medium- to well-sorted pebbly sand and pebble-cobble gravel (unit 8d), massive well-sorted sand (unit 8c), coarse sand and pebble-cobble gravel (unit 8b), and medium-grained sand (unit 8a). This sequence is overlain by loose, massive to crudely stratified cobble to small boulder gravel in a matrix of medium to coarse sand (unit 7).

A moderately to well-indurated, massive, gravelly sand (unit 6) is present only adjacent to the main fault zone. Downslope from the main fault zone, the deposits consist of a series of pebble-cobble gravel and poorly sorted to unsorted, gravelly sand, which contains significant amounts of silt (units 2, 3, 4, and 5). Individual stratigraphic units were distinguished and mapped on the basis of varying amounts and sizes of gravel clasts and on the basis of relatively high amounts of $CaCO_3$ (units 3a and 4a), which gave these units a slightly lighter (whiter) color. The uppermost deposit in the trench (unit 1) is modern slope colluvium, comprised of poorly sorted, silty fine sand, which contains increasing amounts of pebble gravel upslope; this unit is unfaulted. Slope colluvium on alluvial-fan gravels is not typically comprised of silty fine sand; the fine-grained character of this slope colluvium indicates that a significant amount of eolian sediment is being deflated from the playas and exposed pluvial lake sediments and is being deposited across the landscape. Along the lowermost, southwestern parts of the trench, a 5- to 8-cm-thick vesicular A horizon is present at the top of this silty sand deposit (not shown in figure 6).

In this trench, we did not expose correlative stratigraphic units on the hanging wall and the footwall of the fault, which means that the cumulative throw on these Quaternary deposits exceeds the depth of the trench. This lack of correlation indicates a minimum late Quaternary stratigraphic throw on the fault of at least 6.9 m (fig. 6).

Central Trench (CEG)

The CEG trench was excavated across a 6.6-m-high scarp (fig. 10; fig. 5*A*, profile P-5A) on the distal part of an alluvial piedmont, which extends 3–4 km eastward to the foot of the Desatoya Mountains and north of the Eastgate Hills. The trench was located at lat 39°20.994′ N., long 117°51.253′ W. (UTM 11S. 0426397 m E., 4355955 m N.). We exposed three zones of faulting in the trench: (1) a zone of east down-to-the-west normal faults, which is the main fault zone, (2) a zone of fault strands in the middle of the trench that have down-to-the-west displacement, and (3) a west zone of two fault strands that have down-to-the-east displacement. The east and west fault zones define a small graben, which spans most of the trench's length.

Deposits on the upthrown, footwall side of the fault (fig. 11) consist of loose, pebble to cobble gravel (unit 7) overlain by poorly stratified, massive cobble gravel (unit 6). On the

Table 3. Summary of luminescence-dating information for trenches across the Eastgate fault, Nevada.

[See trench maps (figs. 6 and 7) on accompanying map sheet for exact locations of samples; locations were measured using the grids shown on the maps. Estimated ages are based on dose rates that use 15 percent average moisture content through time. IRSL, Infra-red stimulated luminescence; —, data not available; do, ditto]

Field sample number	Trench name, unit number	Location on trench map, horizontal; vertical	Thermoluminescence age (ka)	IRSL age (ka)	Blue-light luminescence age (ka)	Comments
NEGT-TL1	North, 2a	6.7 m; 2.8 m	—	3.22±0.28	—	
NEGT-TL1	do	do	3.15±0.35	—	—	After IRSL/124°C preheat, total bleach
NEGT-TL1	do	do	3.67±0.58	—	—	Partial bleach
NEGT-TL2	North, 3a	10.0 m; 2.4 m	—	4.93±0.45	—	
NEGT-TL2	do	do	—	3.49±0.33	—	
NEGT-TL2	do	do	—	—	4.12±1.53	Very little pure SiO_2
NEGT-TL2	do	do	5.19±1.34	—	—	After IRSL/124°C preheat, total bleach
NEGT-TL3	North, 8c	16.5 m; 3.5 m	—	62.6±5.30	—	Good data
NEGT-TL3	do	do	—	50.1±4.29	—	Good data
NEGT-TL3	do	do	67.8±6.00	—	—	Good data, clear plateau
NEGT-TL3	do	do	56.3±6.54	—	—	Not as good as previous run
TL-CEG1	Central, 1c	5.1 m; 3.1 m	—	4.68±0.40	—	Good data
TL-CEG1	do	do	—	3.29±0.29	—	
TL-CEG1	do	do	4.76±0.52	—	—	After IRSL/124°C, good data, clear plateau, total bleach
TL-CEG1	do	do	4.94±0.47	—	—	Long concise plateau, good data
TL-CEG2	Central, 2	9.0 m 3.1m	—	23.1±2.08	—	Data unreliable and scattered
TL-CEG2	do	do	—	—	6.81±2.34	Very little pure SiO_2
TL-CEG2	do	do	2.76±0.47	—	—	After IRSL/124°C, no silt for further analyses
TL-CEG3	Central, 2	8.9 m; 2.6 m	—	16.4±1.30	—	Good data
TL-CEG3	do	do	—	18.0±1.46	—	Good data
TL-CEG3	do	do	—	21.2±1.69	—	Extended counts, good data
TL-CEG3	do	do	14.0±1.26	—	—	After IRSL/124°C, good data, clear plateau, total bleach
TL-CEG3	do	do	20.9±1.89	—	—	Plateau not as concise as first analysis
TL-CEG3	do	do	14.5±1.73	—	—	Plateau good, stable, extended counts
TL-CEG4	Central, 2	6.6 m; 2.5 m	—	15.9±1.44	—	Large scatter in data
TL-CEG4	do	do	—	21.4±1.77	—	Large scatter in data
TL-CEG4	do	do	—	—	9.59±2.05	Very little pure SiO_2
TL-CEG4	do	do	7.26±1.57	—	—	After IRSL/124°C, excessive scatter in data, two plateaus, total bleach.
TL-CEG4	do	do	12.6±2.91	—	—	After IRSL/124°C, excessive scatter in data but reasonable plateau, total bleach.
TL-CEG5	Central, 5a	7.3 m; 2.2 m	—	12.8±1.21	—	
TL-CEG5	do	do	—	—	2.76±0.82?	Very little pure SiO_2
TL-CEG5	do	do	14.3±9.57	—	—	After IRSL/124°C, excessive scatter in data, total bleach.
TL-CEG6	Central, 5a	8.4 m; 1.5 m	—	22.7±1.84	—	Good data
TL-CEG6	do	do	—	31.8±2.71	—	Good data
TL-CEG6	do	do	—	28.7±2.35	—	Extended counts, good data
TL-CEG6	do	do	18.3±3.90	—	—	After IRSL/124°C, short plateau, reasonable data, total bleach.
TL-CEG6	do	do	28.4±4.21	—	—	After IRSL/124°C, long plateau, good data, total bleach
TL-CEG6	do	do	37.3±3.86	—	—	After IRSL/124°C, two plateaus as in first and second runs, total bleach.

Table 4. Preferred ages of luminescence-dating information for trenches across the Eastgate fault, Nevada.

[See trench maps (figs. 6 and 7) on accompanying map sheet for exact locations of samples; TL, thermoluminescence; IRSL, infra-red stimulated luminescence; OSL, optically stimulated luminescence]

Field sample number	Preferred luminescence age (ka)	Comments
NEGT-TL1	3.3±0.4	Average of three determinations
NEGT-TL2	4.4±0.7	Average of four determinations
NEGT-TL3	59.2±5.5	Average of four determinations; good data from analyses
TL-CEG1	4.4±0.4	Average of four determinations; good data from analyses
TL-CEG2	Unreliable	Inconsistent results from TL, IRSL, and OSL analyses
TL-CEG3	17.5±1.6	Average of six determinations; some scatter but generally consistent results between TL and IRSL results.
TL-CEG4	Unreliable	Large range in age estimates between differing methods; large scatter in data for individual analyses
TL-CEG5	Unreliable	Large range in age estimates between differing methods; large scatter in data for individual analyses
TL-CEG6	27.9±3.1	Average of six determinations; generally good data, but considerable range in individual TL determinations.

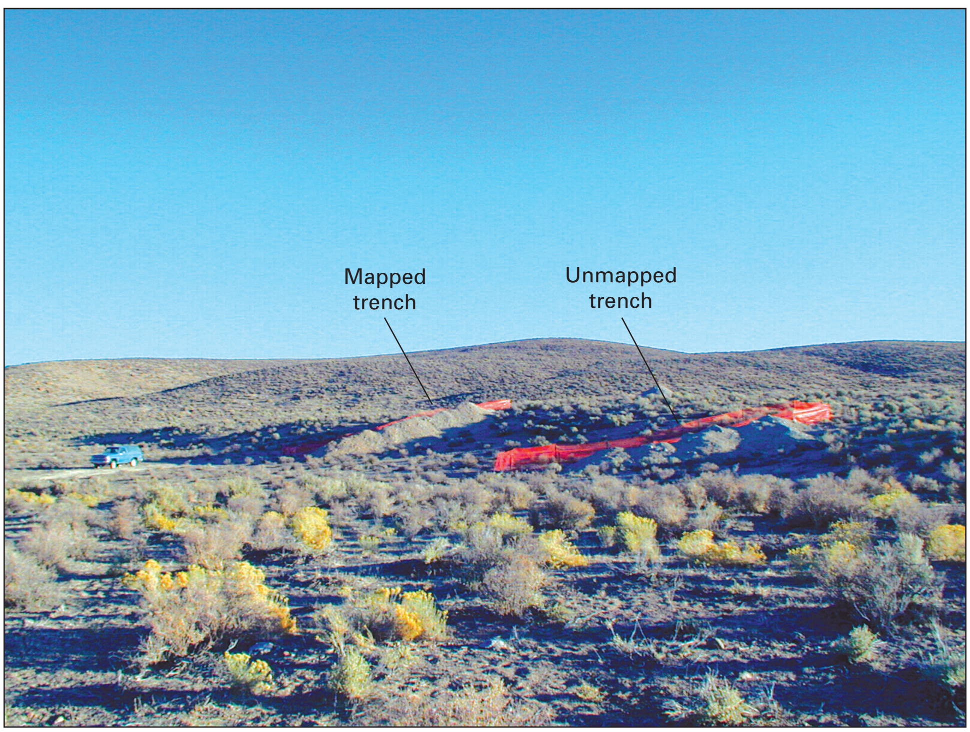

Figure 8. View to the north-northeast of the 5.9-m-high fault scarp at the northern (NEG) trench site. Figure 6 shows the map of the south wall of the mapped trench in left-center of photograph. Trench on the right was not mapped; see text for explanation.

downthrown side of the main fault zone, we mapped a series of massive, pebbly to cobbly, sandy silt and fine-grained sand deposits (units 1, 2, 3, and 4) and a distinctive, slightly fissile, clayey silt and gravelly silt (unit 5). Several of the stratigraphic units on the downthrown side of the fault thin or pinch-out to the west (units 2, 3, 4, and 5b), which is a common characteristic of fault-related colluvial wedges. The uppermost deposit that we mapped in the trench (unit 1) is unfaulted, and, therefore, must postdate the most recent surface rupture on this part of the fault.

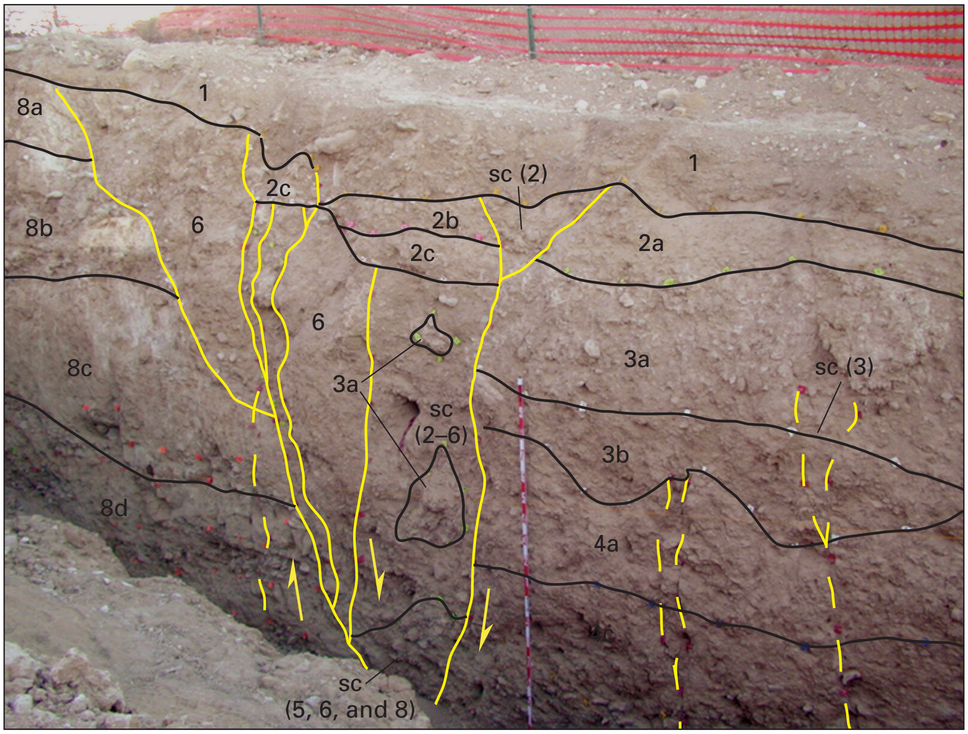

Figure 9. View of part of southeast wall of northern (NEG) trench across Eastgate fault showing traces of major faults and eroded free face (solid yellow lines, arrows indicated sense of movement) in main fault zone, secondary faults or fractures (dashed yellow lines) and stratigraphic units. See figure 6 for map of the entire wall.

Figure 10. View to the east-northeast of the 6.6-m-high fault scarp at the central (CEG) trench site. Orange fencing surrounds the CEG trench.

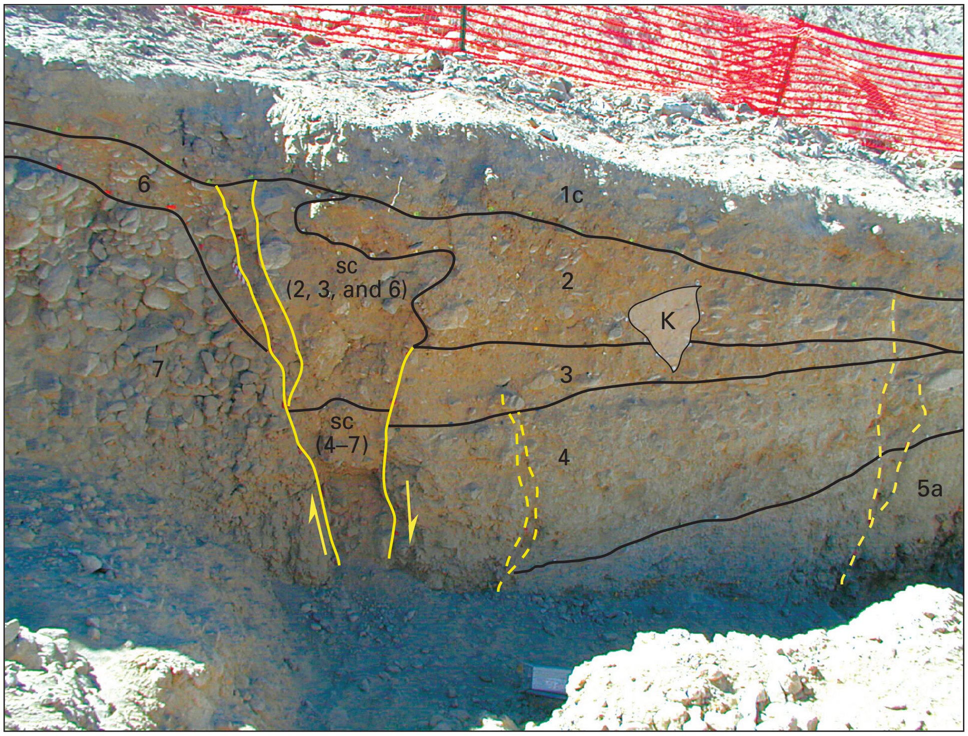

Figure 11. View of part of south wall of central (CEG) trench across the Eastgate fault showing traces of major faults (solid yellow lines, arrows indicate sense of movement), secondary faults or fractures (dashed yellow lines) and stratigraphic units. K, krotovina (bioturbated sediment). See figure 7 for map of the entire wall.

The precise correlation of units across the fault is somewhat uncertain. The similarity of the cobble gravels that we mapped as unit 7 on the footwall and hanging wall suggests a direct correlation, but it is also possible that the gravel of unit 6 could correlate with unit 7 in the hanging wall. This ambiguity in correlations results in two measurements of minimum stratigraphic throw on the fault (fig. 7). If the deposits labeled as unit 7 in figure 7 correlate, then the minimum stratigraphic throw is 5.0 m. If unit 6 in the footwall correlates with unit 7 in the hanging wall, then the minimum stratigraphic throw is 6.4 m.

Summary

Our detailed trench maps and the related chronologic information from two trenches across the Eastgate fault are the basic data needed to clarify the history of Quaternary movement on the fault. Geomorphic relations on the landscape and the stratigraphy in the trenches both indicate that surface ruptures have occurred on the fault at several times in the latter part of the Quaternary (that is, late Pleistocene to Holocene time). The moderately strong soil development in the alluvial deposits that we trenched suggests that the 5- to 6-m-high scarps at the two trench sites record a faulting history that extends back in time at least tens of thousands of years. A more complete interpretation of the field and laboratory data presented here will offer new insight into the long-term behavior of the Eastgate fault, and when combined with similar information from studies of other faults in the region, will provide an important perspective on the temporal and spatial pattern of Quaternary faulting in and around this part of the Central Nevada seismic belt.

References Cited

Bell, John, and Katzer, Terry, 1990, Timing of late Quaternary faulting in the 1954 Dixie Valley earthquake area, central Nevada: Geology, v. 18, p. 622–625.

Bell, J.W., dePolo, C.M., Ramelli, A.R., Sarna-Wojcicki, A.M., and Meyer, C.E., 1999, Surface faulting and paleoseismicity of the 1932 Cedar Mountain earthquake area, west-central Nevada, and implications for modern tectonics of the Walker Lane: Geological Society of America Bulletin, v. 111, no. 6, p. 791–807.

Bennett, R.A., Wernicke, B.P., and Davis, J.L., 1998, Continuous GPS measurements of contemporary deformation across the Basin and Range province: Geophysical Research Letters, v. 25, p. 563–566.

Birkeland, P.W., 1999, Soils and geomorphology (3d ed.): New York, Oxford University Press, 430 p.

Bucknam, R.C., and Anderson, R.E., 1979, Estimation of fault-scarp ages from a scarp-height–slope-angle relationship: Geology, v. 7, p. 11–14.

Caskey, S.J., Wesnousky, S.G., Zhang, P., and Slemmons, D.B., 1996, Surface faulting of the 1954 Fairview Peak (Ms 7.2) and Dixie Valley (Ms 6.9) earthquakes, central Nevada: Bulletin of the Seismological Society of America, v. 86, no. 3, p. 761–787.

dePolo, C.M., 1998, A reconnaissance technique for estimating the slip rates of normal-slip faults in the Great Basin, and application to faults in Nevada, U.S.A.: Reno, Nev., University of Nevada-Reno Ph.D. dissertation, 199 p., 5 appendices.

dePolo, C.M., Clark, D.G., Slemmons, D.B., and Ramelli, A.R., 1991, Historical surface faulting in the Basin and Range province, western North America—Implications for fault segmentation: Journal of Structural Geology, v. 13, no. 2, p. 123–136.

Dohrenwend, J.C., Schell, B.A., and Moring, B.C., 1992, Reconnaissance photogeologic map of young faults in the Millett 1° by 2° quadrangle, Nevada: U.S. Geological Survey Miscellaneous Field Studies Map MF–2176, scale 1:250,000.

Kollmorgen Instruments Corp. (Macbeth Division), 1994, Munsell Soil Color Charts (revised ed.): New Windsor, N.Y., unpaginated, [405 Little Britain Rd., New Windsor, N.Y. 12553].

Machette, M.N., 1989, Slope-morphometric dating, *in* Forman, S.L., ed., Dating methods applicable to Quaternary geologic studies in the western United States: Utah Geological and Mineral Survey Miscellaneous Publication 89–7, p. 30–42.

Machette, M.N, 2005, Summary of the late Quaternary tectonics of the Basin and Range province in Nevada, Eastern California, and Utah, *in* Lund, W.R., ed., Proceedings Volume, Basin and Range Province Seismic Hazards Summit II, Western States Seismic Policy Council, Reno, Nev., May 16–91, 2004: Utah Geological Survey Miscellaneous Publication 05-2 (CD-ROM), 18 p.

Machette, M.N., Haller, K.M., Ruleman, C.A., Mahan, S.A., and Okumura, Koji, 2005, Geologic evidence for late Quaternary movement on the Clan Alpine fault, west-central Nevada—Trench logs, scarp profiles, location maps, and sample and soil descriptions: U.S. Geological Survey Scientific Investigations Map 2891, 1 oversize plate. [Available at: http://pubs.usgs.gov/sim/2005/2891/].

Mayer, Larry, 1984, Dating Quaternary fault scarps formed in alluvium using morphologic parameters: Quaternary Research, v. 22, p. 300–313.

McKee, E.D., and Stewart, J.H., 1971, Stratigraphy and potassium-argon ages of some Tertiary tuffs from Lander and Churchill Counties, central Nevada: U.S. Geological Survey Bulletin 1311–B, 28 p.

Personius, S.F., Anderson, R.E., Okumura, Koji, Mahan, S.A., and Hancock, D.A., 2004, Log and data from an investigation of the Orovada trench site, Santa Rosa Range fault zone, Humboldt County, Nevada: U.S. Geological Survey Scientific Investigations Map 2815, 1 oversize plate. [Available at: http://pubs.usgs.gov/sim/2004/2815/].

Pierce, K.L., and Colman, S.M., 1986, Effect of height and orientation (microclimate) on geomorphic degradation rates and processes, late-glacial terrace scarps in central Idaho: Geological Society of America Bulletin, v. 97, p. 869–885.

Stewart, J.H., and Carlson, J.E., 1976, Geologic map of north-central Nevada: Nevada Bureau of Mines and Geology Map 50, scale 1:250,000.

Stewart, J.H., Sarna-Wojcicki, Andrei, Meyer, C.E., Starratt, S.W., and Wan, Elmira, 1999, Stratigraphy, tephrochronology, and structural setting of Miocene sedimentary rocks in the Middlegate area, west-central Nevada: U.S. Geological Survey Open-File Report 99–350, 17 p., 1 oversize plate, scale 1:24,000.

Thatcher, W., Goulger, G.R., Julian, B.R., Svarc, J., Quilty, E., and Bawden, G.W., 1999, Present-day deformation across the Basin and Range province, western United States: Science, v. 283, p. 1714–1718.

Wallace, R.E., 1977, Profiles and ages of young fault scarps, north-central Nevada: Geological Society of America Bulletin, v. 88, p. 1267–1281.

Wallace, R.E., 1984a, Patterns and timing of late Quaternary faulting in the Great Basin province and relation to some regional tectonic features: Journal of Geophysical Research, v. 89, no. B7, p. 5763–5769.

Wallace, R.E., 1984b, Faulting related to the 1915 earthquakes in Pleasant Valley, Nev.: U.S. Geological Survey Professional Paper 1274–A, 33 p.